J Fluoresc (2015) 25:1921–1929
DOI 10.1007/s10895-015-1684-0

ORIGINAL ARTICLE

# A Novel $Cr^{3+}$ Fluorescence Turn-On Probe Based on Rhodamine and Isatin Framework

**Anamika Dhara**[1] · **Nikhil Guchhait**[1] · **Susanta K. Kar**[1]

Received: 23 July 2015 / Accepted: 28 September 2015 / Published online: 15 October 2015


**Abstract** A novel turn-on fluorescent dye (E)-3′,6′-bis(diethylamino)-2-((1-(naphthalen-2-ylmethyl)-2-oxoindolin-3-ylidene)amino)spiro[isoindoline-1,9′-xanthen]-3-one (**RBNI**) based on a rhodamine-isatin hybrid molecular architecture was synthesized by condensation of isatin derivative with rhodamine hydrazide. The dye **RBNI** is selective and sensitive for recognition of $Cr^{3+}$ ion in aqueous $CH_3CN$ media over other tested metal ions. The sensor shows large fluorescence enhancement upon complexation with $Cr^{3+}$ and simultaneous color change occurs from colorless to pink-red. Spectroscopic study predicted 1:1 binding stoichiometry between **RBNI** and $Cr^{3+}$ ion and this was again verified through ESI-MS (Electrospray Ionisation Mass Spectrometry). Detection limit of $Cr^{3+}$ ion by this dye was calculated to be 2.4 μM. Furthermore, the potential application of this dye for the monitoring of $Cr^{3+}$ ions in pond water and tap water samples was demonstrated.

**Keywords** Chemosensor · $Cr^{3+}$ ion · Fluorescence · Job's plot · Rhodamine derivative

**Electronic supplementary material** The online version of this article (doi:10.1007/s10895-015-1684-0) contains supplementary material, which is available to authorized users.

✉ Nikhil Guchhait
nguchhait@yahoo.com

✉ Susanta K. Kar
skkar_cu@yahoo.co.in

[1] Department of Chemistry, University College of Science, University of Calcutta, 92, A.P.C. Road, Kolkata 700 009, India

## Introduction

Fluorescent sensing via suitable sensors is an attractive and efficient chemical tool because of its high sensitivity, selectivity, and simple instrumentation [1–5]. Fluorescent sensors could be considered as molecular receptors that convert their fluorescent messages into analytically useful signals upon binding to specific guests [6]. Chromium (III) is an essential micronutrient required in amounts of 50–200 μg per day for humans and animals [7]. It affects human metabolism by modulation of the action of insulin through glucose tolerance factors (GTF), thereby activating certain enzymes and stabilizing proteins and nucleic acids [8–11]. Insufficient intake of $Cr^{3+}$ increases the risk for diabetes and cardiovascular diseases including elevated levels of circulating insulin, glucose, triglycerides and total cholesterol, and impaired immune function [12]. However, higher concentration of $Cr^{3+}$ is detrimental to cellular functions and structures [13]. Serious environmental pollution can be caused due to the discharge of chromium by industrial and other activities. Due to its biological impact, the United States Environmental Protection Agency (USEPA) has set strict standards on the permissible concentration of $Cr^{3+}$ in natural water (0.1 mg $mL^{-1}$) in an attempt to control build-up due to industrial and agricultural activities [14, 15]. At the same time, the higher oxidation state of Cr (VI) is an extremely toxic and potentially carcinogenic. It can penetrate through cell membranes and causes toxic effects including cancer by oxidizing DNA and some proteins [16–18]. Thus, there is need for the development of sensitive and selective way for $Cr^{3+}$ ions detection of environmental and biological samples. Current approaches for environmental and clinical samples rely on costly, time-consuming methods like atomic absorption/emission spectroscopy [19] or inductively coupled plasma mass spectrometry [20] which are not very convenient and handy for "in-field" detection. These limitations have

actually set off an interest among chemists for the development of efficient, cost-effective, and reversible chemosensors for $Cr^{3+}$ ion. Generally a 'turn-off' response, i.e., fluorescence quenching is observed in sensing events due to paramagnetic tendency of $Cr^{3+}$ ion [21]. There are very limited reports where a 'turn-on' response has been reported for sensing of $Cr^{3+}$ ion and the fluorescence enhancement were reported to be about 15 to 30 folds [22–25]. Whereas, fluorescence quenching is not conductive to a high signal output upon recognition and interferes with temporal separation of similar complexes with time-resolved fluorometry [26]. Hence, the sensors with "turn-on" fluorescence response are more attractive than the "turn-off" ones as they offer the potential for high sensitivity [27–29]. During the last decade, a few numbers of fluorescent probes have been reported for the purpose of $Cr^{3+}$ sensing. However, there are several shortcomings such as cross-sensitivity toward other metal cations, lack of selective multi-chelating ligand, low water solubility, slow response, low fluorescence enhancement and cytotoxicity. It is apparent that there is a need to design new fluorescent probes for chromium ions which can overcome these limitations. For these reasons, we have taken care to design an isatin-appended rhodamine based scaffold as a chemosensor. Rhodamine dyes are extensively employed in the study of complex biological systems as molecular probes because of their high absorption coefficients, high fluorescence quantum yields, and long wavelength absorption and emission [30]. These unique properties make rhodamine dyes a good candidate in constructing a "turn-on" fluorescent probe for $Cr^{3+}$ ion [31]. Incorporation of isatin moiety into a rhodamine-based system makes our probe more promising because of their strong binding affinity towards metals. Isatin and its derivatives are potent inhibitors of monoamine oxidase, caspase-3 and so on [32, 33].

In the present work, we have synthesized new dyad **RBNI**, where in the fluorophore rhodamine core is linked to an isatin derivative which acts as a soft metal chelating site, to achieve the *"off-on"* type fluorescence enhanced sensing protocol based upon coordination method. The hallmark of its superiority over the reported methods is, the ease of synthesis as well as very low detection limit (2.4 μM) observed during the selective detection of $Cr^{3+}$. We anticipated that **RBNI** binds to $Cr^{3+}$ ion result in the fluorescence enhancement [34–38]. Chelation-enhanced fluorescence (CHEF) [34–37] can be possible in presence of metal ion as CHEF is an attractive design principle for developing luminescent chemical devices, which combine the ability to recognize and respond to an external input mostly with photoinduced electron transfer (PET) process. Upon complexation of ligand with a certain metal ion, a large fluorescence enhancement can be observed because the stable chelation abrogates the PET process from the electron donating group to the fluorophore ("turn-on state"). In some cases binding of metal to a flexible ligand causes decrease of non-radiative decay channels of energy dissipation causing enhancement of fluorescence upon binding. The data obtained from fluorimetric titration and competition experiments indicate that **RBNI** is pH-stable and highly selective towards $Cr^{3+}$ over other metal ions. As far as our knowledge is concerned, this is one of the rare examples of a rhodamine derivative employed for the selective detection of $Cr^{3+}$.

## Experimental

### Synthesis

#### *Synthesis of Compound* **3**

Indoline-2,3-dione (1 g, 6.79 mmol) was dissolved in DMF (15 mL) and treated with cesium carbonate (3.54 g, 10.86 mmol) and 1-(bromomethyl)naphthalene (1.99 g, 9.03 mmol). The mixture was stirred at ambient temperature for 2 days. The reaction mixture was quenched with ice and then extracted with ethyl acetate and finally washed with brine (100 mL×3), then dried over sodium sulphate and concentrated under reduced pressure to give an orange solid product. Yield: 0.8 g, 40 %. IR (KBr, $cm^{-1}$) 400–4000: υ=3447, 2924, 2364, 1729, 1607, 1465, 1338, 1171, 1089, 1022, 862, 812, 753, 466; $^1$H-NMR (500 MHz, $CDCl_3$): δ (ppm), 5.10 (s, 2H, $-CH_2$-), 6.82 (d, 1H, naph-H, *J*=7.9 Hz), 7.09 (d, 1H, Ar-H, *J*=5 Hz), 7.50–7.42 (m, 4H, naph-H & Ar-H), 7.63 (d, 1H, naph-H, *J*=7.3 Hz), 7.85–7.79 (m, 4H, naph-H & Ar-H); Anal. Calc. for $C_{19}H_{13}NO_2$: C, 79.53; H, 4.58; N, 4.89; Found: C, 79.43; H, 4.56; N, 4.88.

#### *Synthesis of Compound* **RBNI**

Rhodamine B hydrazide (**5**) was prepared according to the literature procedure as described previously and was characterized by $^1$H NMR, mass data and FT-IR [39, 40]. Rhodamine B hydrazide (0.5 g, 1.095 mmol) was dissolved in 10 mL ethanol and 1-(naphthalen-1-ylmethyl)indoline-2,3-dione (0.31 g, 1.095 mmol) was added. The mixture was then heated under reflux condition for 6 h. After completion of the reaction, a yellow precipitate was formed within the reaction flask (Scheme 1). Then, it was cooled and the resulting precipitate was filtered off, washed with methanol/ether (1:1) by three times and dried under vacuum. Yield: 0.25 g, 31 %. M.P.−231 °C (decomp.). IR (KBr, $cm^{-1}$) 400–4000: υ= 3062, 2926, 1701, 1613, 1516, 1468, 1542, 1263, 1219, 1117, 817, 782; $^1$H-NMR (500 MHz, DMSO-$d_6$): δ (ppm), 1.10 (t, 12H, $NCH_2\underline{CH_3}$, *J*=6.7 Hz), 3.33 (q, 8H, $N\underline{CH_2}CH_3$, *J*=5 Hz), 5.10 (s, 2H,-$CH_2$-), 6.41–6.36 (m, 4H, xanthene-H), 6.98 (s, 2H, xanthene-H), 7.06 (d, 1H, isatin Ar-H, *J*=7.4 Hz), 7.12 (d, 1H, naph-H, *J*=7.4 Hz), 7.31 (d, 1H, naph-H, *J*= 7.2 Hz), 7.36 (s, 1H, isatin Ar-H), 7.45 (d, 1H, naph-H, *J*=

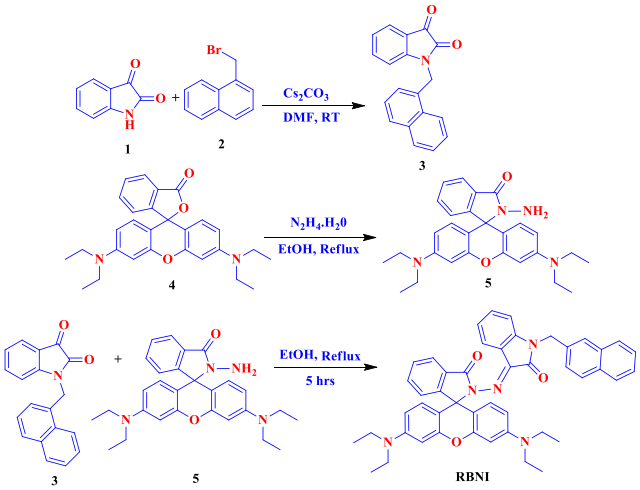


**Scheme 1** Synthesis of chemosensor **RBNI**

8.2 Hz), 7.52–7.50 (m, 1H, Ar-H), 7.57 (s, 2H, Ar-H), 7.61 (s, 2H, naph-H), 7.95–7.88 (m, 5H, Ar-H, isatin Ar-H & naph-H); ESI-MS: *m/z* calculated for $C_{47}H_{43}N_5O_3$ $[M+H]^+$ 726.34, found 727; Anal. Calc. for $C_{47}H_{43}N_5O_3$: C, 77.79; H, 5.99; N, 9.64; Found: C, 77.77; H, 5.97; N, 9.65.

*Synthesis of* **RBNI**-$Cr^{3+}$ *Complex*

A 5 mL methanolic solution of $CrCl_3$ (0.010 g, 0.0688 mmol) was added drop wise to a magnetically stirred solution of **RBNI** (0.05 g, 0.0688 mmol) in methanol (5 mL). The colour of the ligand solution was changed from almost colorless to pink-red upon addition $CrCl_3$. After 2 h of stirring at room temperature, the solution was dried using rotary evaporator which yielded a pink-red **RBNI**-$Cr^{3+}$ complex. The complex was characterized by $^1$H NMR, MS and FT-IR studies.

## Materials and Instruments

All other chemicals used were of analytical grade. The solutions of metal ions were prepared from their perchlorate salts. All solvents used in spectroscopic tests were of spectrostropic grade. Distilled-deionized water was used throughout the experiment. A Perkin Elmer (Model LS-50B) fluorimeter was used for fluorescence measurements. The absorption spectra were recorded with a Hitachi model U-3501 spectrophotometer. NMR spectra were recorded on a Bruker spectrometer at 500 ($^1$H NMR) MHz in DMSO-$d_6$. Chemical shifts (δ values) were reported in ppm down field from internal $Me_4Si$. Elemental analyses were carried out with a Perkin–Elmer CHN analyzer 2400 instrument. Mass spectra were recorded in methanol solvent in Qtof Micro YA263. IR spectra (KBr pellet, 400–4000 $cm^{-1}$) were recorded on a Perkin–Elmer model 883 infrared spectrophotometer. Melting points were determined using a Buchi 530 melting apparatus. Fluorescence lifetimes were measured by the method of Time Correlated Single-Photon Counting (TCSPC) using a HORIBA JobinYvon Fluorocube-01-NL fluorescence lifetime spectrometer. The sample was excited using a nanosecond laser diode at 340 nm and the signals were collected at the magic angle of 54.7° to eliminate any considerable contribution from fluorescence anisotropy decay [41]. The typical time resolution of the experimental set-up is~800 ps. The decays were deconvoluted using DAS-6 decay analysis software. The acceptability of the fits was judged by $\chi^2$ criteria and visual inspection of the residuals of the fitted function to the data. Mean (average) fluorescence lifetimes were calculated using the following Eq. (1):

$$\tau_{av} = \frac{\sum \alpha_i \tau_i^2}{\sum \alpha_i \tau_i} \quad (1)$$

in which $\alpha_i$ is the pre-exponential factor corresponding to the ith decay time constant, $\tau_i$.

## General Method of UV-vis and Fluorescence Titration

Stock solutions of the probe **RBNI** were prepared in 50 % (*v/v*) $H_2O/CH_3CN$ buffered by 10 mM HEPES pH 7.2, in the concentration range $10^{-5}$ M. 2 mL of the receptor solution was taken in a cuvette. Stock solutions of guests in the concentration range $2\times10^{-5}$ M were prepared in the same solvents and were individually added in different amounts to the receptor solution. The same stock solutions for the receptor and guests were used to perform the UV-vis and fluorescence titration experiments. Both fluorescence and UV-vis titration experiments were carried out at 25 °C. Fluorescence measurements were carried out with excitation and emission slit of 2.5 and 2.5 nm ($\lambda_{ex}$=530 nm).

## Quantum Yield Measurements

The fluorescence quantum yields were determined using rhodamine 6G as a reference [42] with a known $\Phi_R$ value of 0.95 in EtOH. The area of the emission spectrum was integrated using the software available in the instrument and quantum yield was calculated according to the following equation [43]:

$$\Phi_S/\Phi_R = [A_S/A_R] \times \left[(Abs)_R/(Abs)_S\right] \times \left[\eta_S{}^2/\eta_R{}^2\right] \quad (2)$$

where $\Phi_S$ and $\Phi_R$ are the fluorescence quantum yield of the sample and reference, respectively; $A_S$ and $A_R$ are the area under the fluorescence spectra of the sample and the reference, respectively; $(Abs)_S$ and $(Abs)_R$ are the corresponding optical densities of the sample and the reference solution at the wavelength of excitation; $\eta_S$ and $\eta_R$ are the refractive index of the sample and the reference, respectively.

### Calculation of the Detection Limit

The detection limit (DL) of **RBNI** for $Cr^{3+}$ was determined using the following equation:

$$DL = K \times Sb / S \quad (3)$$

Where $K$=2 or 3 (we take 3 in this case), Sb is the standard deviation of the blank solution and S is the slope of the calibration curve.

## Results and Discussion

### Design and Synthesis of RBNI

Rhodamine B hydrazide was synthesized according to a previous report [39, 40]. The synthesis of **RBNI** is depicted in Scheme 1. Sensor **RBNI** was synthesized by simple Schiff-base condensation between rhodamine B hydrazide (**5**) and 1-(naphthalen-1-ylmethyl)indoline-2,3-dione (**3**) in methanol and thoroughly characterized by $^{1}H$ NMR, $^{13}C$ NMR, ESI-$MS^{+}$, FT-IR and CHN elemental analysis (Figs. S1–S6, in Supplementary data).

### UV–vis and Fluorescence Studies

Steady state absorption and fluorescence spectra were recorded to investigate spectroscopic changes of probe **RBNI** (10 μM) in presence of various metal ions in 50 % (*v/v*) $H_2O/CH_3CN$ buffered by 10 mM HEPES, pH 7.2 at 25 °C. As shown in Fig. 1, the absorption spectra of **RBNI** exhibited only a very weak band over 500 nm region, indicating that the rhodamine core is in the ring closed isomeric form. Addition of $Cr^{3+}$ into this solution immediately resulted in a significant enhancement of absorbance (about 40 fold) in the visible range of 500–600 nm and a new peak at 560 nm was observed. With increasing $Cr^{3+}$ ion concentration, a shoulder peak at ~520 nm is also observed. The absorbance of **RBNI** at 560 nm was proportional to $Cr^{3+}$ ion concentration over a range of 0-45 μM. The colour of the solution changed from colorless to pink-red upon titration with $Cr^{3+}$ ions which may be due to opening of spirolactum ring of the rhodamine moiety. The absorbance at 560 nm as a function of $Cr^{3+}$ concentration is depicted in inset Fig. 1. Addition of separately 45 μM each of other metal ions viz., $Na^{+}$, $K^{+}$, $Mg^{2+}$, $Mn^{2+}$, $Co^{2+}$, $Ni^{2+}$, $Ga^{3+}$, $In^{3+}$, $Zn^{2+}$, $Cd^{2+}$ and $Hg^{2+}$, did not perturb the UV-visible spectral pattern of **RBNI** to a significant extent (Fig. S7 in Supplementary data). However $Fe^{3+}$, $Cu^{2+}$, $Al^{3+}$ and $Pb^{2+}$ did affect to an extent by changing of absorbance and slight blue shifting of the absorption band with respect to the band observed in presence of $Cr^{3+}$ ion. In these four cases the colour of the **RBNI** categorically became light pink. Thus it was not possible to discriminate any single metal ion through **RBNI** only by UV-visible spectral changes. Moreover, when being excited by 365 nm UV lamp it emits orange lights only in case of $Cr^{+3}$ ion, which acts as a typical "OFF-ON" based optical response (Fig. 2).

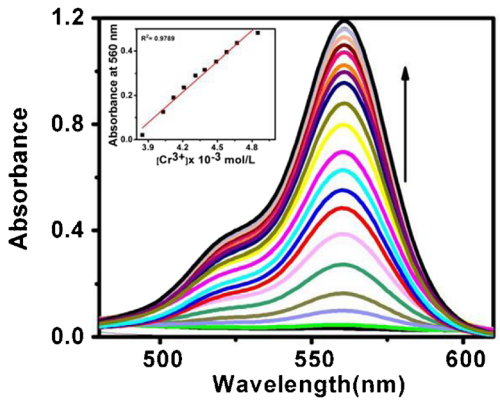


**Fig. 1** UV-vis spectra of chemosensor **RBNI** (10 μM) in 50 % (*v/v*) $H_2O/CH_3CN$ buffered by 10 mM HEPES at pH 7.2 at 25 °C, in the presence of different amount $Cr^{3+}$. [$Cr^{3+}$]: 0, 2.5, 5, 7.5, 10, 12.5, 15, 17.5, 20, 22.5, 25, 27.5, 30, 32.5, 35, 37.5, 40, 42.5, 45 μM. Insert: absorbance at 560 nm as a function of $Cr^{3+}$ concentration

The fluorescence spectrum of chemosensor **RBNI** (10 μM) exhibited very weak fluorescence emission (quantum yield, [44, 45] $\Phi$=0.03) when excited at 530 nm in 50 % (*v/v*) $H_2O/CH_3CN$ buffered by 10 mM HEPES, pH 7.2 at 25 °C. As seen in Fig. 3, upon addition of only $Cr^{3+}$ ions to the solution of **RBNI** a remarkable enhancement of emission intensity was observed at 590 nm ($\Phi$=0.36). Fluorescence enhancement observed for **RBNI** in the presence of $Cr^{3+}$ ions is ascribed to be the formation of the **RBNI**-$Cr^{3+}$ complex. The generated complex shows strong emission at 590 nm due to ring opening of the spirolactam ring which causes fluorescence enhancement (~65 fold) by the generation of free rhodamine unit in the complex (Scheme 2). In addition, binding of metal ion insists rigid structure at the binding site of the complex which expected to reduce non-radiative channels causing fluorescence enhancement. Thus, 'Turn-On' of fluorescence with addition of $Cr^{3+}$ ions indicates high selectivity of **RBNI** towards $Cr^{3+}$ ions.

Under the same conditions as was used for $Cr^{3+}$, we also tested the fluorescence behaviour of **RBNI** (10 μM) toward other metal ions ($Na^{+}$, $K^{+}$, $Mg^{2+}$, $Mn^{2+}$, $Co^{2+}$, $Ni^{2+}$, $Ga^{3+}$, $In^{3+}$, $Zn^{2+}$ and $Cd^{2+}$). Very mild fluorescence enhancement factors (FEF) were also detected for $Al^{3+}$ (~17 fold), $Fe^{3+}$ (~8 fold), $Pb^{2+}$ (~6 fold), and $Hg^{2+}$ (~4 fold), and other metal ions showed nearly no response (Fig. 4). These findings indicated that **RBNI** behaved as a highly sensitive and selective fluorescent chemosensor towards $Cr^{3+}$. Relative fluorescence enhancement of **RBNI** in the absence and presence of various other metal ions and thereby its selectivity for $Cr^{3+}$ was shown in Fig. 5.

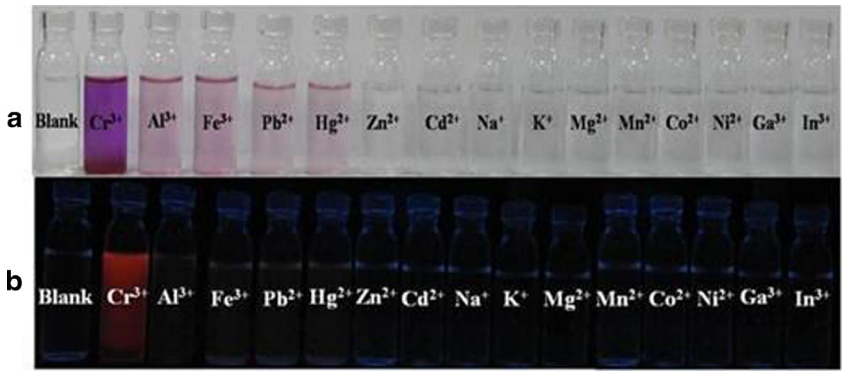


**Fig. 2** Photographs of chemosensor **RNBI** (10 μM) in 50 % (*v/v*) $H_2O/CH_3CN$ buffered by 10 mM HEPES at pH 7.2 at 25 °C, in the presence of different metal ions (100 μM) under **a** visible light **b** UV light

The cross-sensitivity of any probe towards different metal ions limits its utility in selective detection of a metal ion, and that has also been tested with this probe. We also carried out competitive experiments in the presence of $Cr^{3+}$ at 100 μM mixed with $Na^+$, $K^+$, $Mg^{2+}$, $Mn^{2+}$, $Co^{2+}$, $Ni^{2+}$, $Ga^{3+}$, $In^{3+}$, $Zn^{2+}$ and $Cd^{2+}$ $Fe^{2+}$, $Zn^{2+}$, $Hg^{2+}$, $Cu^{2+}$, $Pb^{2+}$, $Ni^{2+}$, $Co^{2+}$, $Cd^{2+}$, $Mg^{2+}$, $Na^+$, $K^+$ at 100 μM. As shown in Fig. 6, no significant variation in the fluorescence spectra of **RNBI** was observed with any other metal ion except $Cu^{2+}$ and $Fe^{3+}$ which induce similar fluorescence emission but to a small extent. Most likely, the paramagnetic nature of these ions ($Cu^{2+}$ and $Fe^{3+}$) is responsible for quenching of fluorescence of the resulting **RBNI** complexes.

The response of **RNBI** with $Cr^{3+}$ ion obtained from different chromium salts such as chromium sulfate, chromium nitrate and chromic chloride were also investigated when addition of $Cr^{3+}$ (10 mM, 50 mM, 100 mM, respectively) to chemosensor **RBNI** (10 μM), the response of **RNBI** with the $Cr^{3+}$ from chromic chloride was in accorded with the $Cr^{3+}$ from other chromium salts (Fig. S8 in Supplementary data). For practical application, the detection limit [46] of **RBNI** was also estimated. The fluorescence titration profile of **RBNI** (10 μM) with $Cr^{3+}$ demonstrated that the detection limit of $Cr^{3+}$ is 2.4 μM [47, 48] . The obtained detection limit was quite lower than the recommended maximum contaminant level (MCL) for chromium in the drinking water ($1.9\times10^{-6}$ M, 0.1 mg/L) defined by the U.S. Environmental Protection Agency (EPA) [49], suggesting that **RBNI** has high specificity toward $Cr^{3+}$ under current working conditions. (Fig. S9, in Supplementary data).

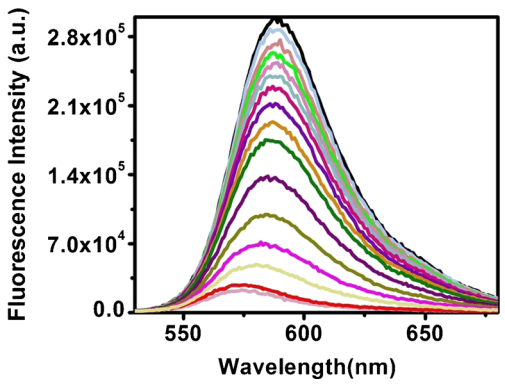


**Fig. 3** Emission spectra of chemosensor **RBNI** (10 μM) in the presence of increasing concentrations of $Cr^{3+}$ (0, 15, 25, 30, 35, 40, 45, 50, 55, 60, 65, 70, 75, 80, 100 μM) in 50 % (*v/v*) $H_2O/CH_3CN$ buffered by 10 mM HEPES at pH 7.2 at 25 °C. Excitation was performed at 530 nm

For the determination of the stoichiometry the complex between **RBNI** and $Cr^{3+}$, Job's plot [50] analysis was also carried out. When molar fraction of $Cr^{3+}$ was 0.5, the absorbance at 560 nm band reaches to maximum (Fig. 7), indicating the formation of 1:1 complex between **RBNI** and $Cr^{3+}$. It also corroborated with the results obtained by TOF MS $ESI^+$ mass spectroscopy in which the peak at m/z 902.72 in the mass spectrum is assigned to the mass of [(**RBNI** + $Cr^{3+}$ + $2Cl^-$ + $3H_2O$)] (Fig. S10, in Supplementary data). This is also confirmed by the Benesi-Hildebrand method [51]. When assuming a 1:1 association between **RBNI** and $Cr^{3+}$, the Benesi-Hildebrand equation is given as follows:

$$1/(A-A_0) = 1/\{K(A_{max}-A_0)[C]\} + 1/(A_{max}-A_0)$$

$A_0$ is the absorbance of **RBNI** at absorbance maxima ($\lambda$= 560 nm), $A$ is the observed absorbance at that particular wavelength in the presence of a certain concentration of the metal ion (C), $A_{max}$ is the maximum absorbance value that was obtained at $\lambda$=560 nm during titration with varying [C], $K$ is the association constant ($M^{-1}$). As shown in Fig. S11 in Supplementary data, the plot of $1/(A–A_0)$ against $1/[Cr^{3+}]$ shows a liner relationship, indicating that **RBNI** indeed associates with $Cr^{3+}$ in a 1:1 stoichiometry. The association constant, $K$, between **RBNI** and $Cr^{3+}$, is determined from the slope to be $3.4\times10^3$ $M^{-1}$.

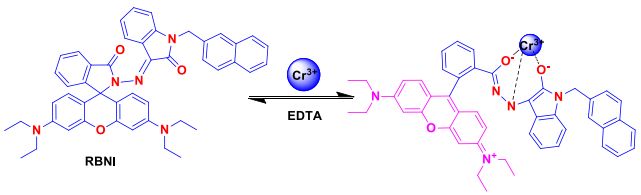


**Scheme 2** Proposed binding mode of **RBNI** with $Cr^{3+}$

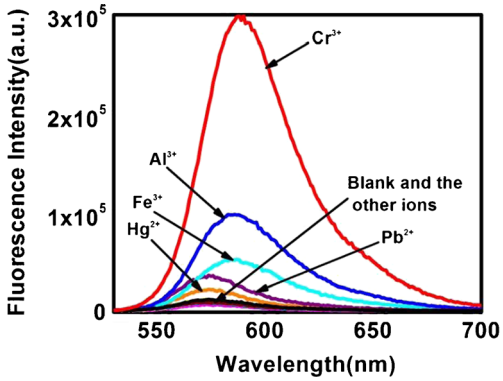


**Fig. 4** Fluorescence spectra (excitation at 530 nm) of **RBNI** (10 μM) in 50 % (*v/v*) $H_2O/CH_3CN$ buffered by 10 mM HEPES at pH 7.2 at 25 °C, by addition of 100 μM different metal ions ($Na^+$, $K^+$, $Mg^{2+}$, $Pb^{2+}$, $Al^{3+}$, $Cr^{3+}$, $Mn^{2+}$, $Fe^{3+}$, $Co^{2+}$, $Ni^{2+}$, $Cu^{2+}$, $Ga^{3+}$, $In^{3+}$, $Zn^{2+}$, $Cd^{2+}$, $Hg^{2+}$)

Since reversibility is a prerequisite in developing chemosensors for practical applications, we also studied the reversibility of the sensing protocol as proposed. The **RBNI**-$Cr^{3+}$ complex was titrated with EDTA to determine the nature of binding. As seen in the Fig. S12, in Supplementary data, with the increase of the concentration of EDTA, the fluorescence intensity at 590 nm gradually decreased. Excess EDTA completely quenched the fluorescence at 590 nm. This observation predicts the removal of $Cr^{3+}$ ion from **RBNI**, leading to the reconstitution of the spirolactam ring in the rhodamine moiety and hence fluorescence at 590 nm vanishes.

## TCSPC Study

The $Cr^{3+}$ recognition has been further supported by measuring the fluorescence life-time of the species by time-correlated single photon counting (TCSPC) technique during the titration. Fig. 8 represents the time resolved fluorescence decay profile of **RBNI** and its metal complex in aqueous $CH_3CN$ media using a 340 nm nano-LED as the excitation source. The TCSPC data

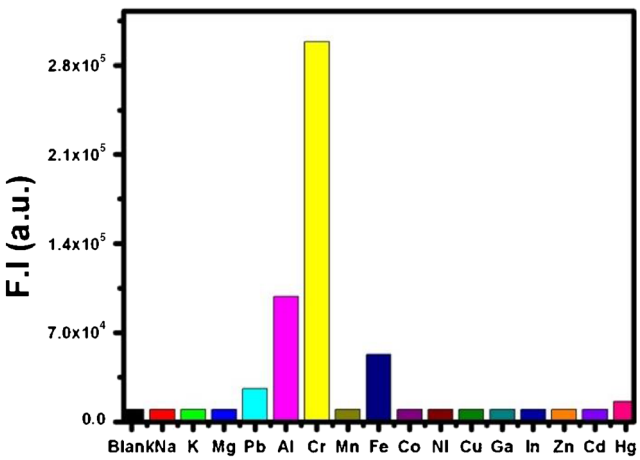


**Fig. 5** *Bar graph* shows the relative emission intensity of **RBNI** at 590 nm upon treatment with various metal ions in 50 % (*v/v*) $H_2O/CH_3CN$ buffered by 10 mM HEPES at pH 7.2 at 25 °C

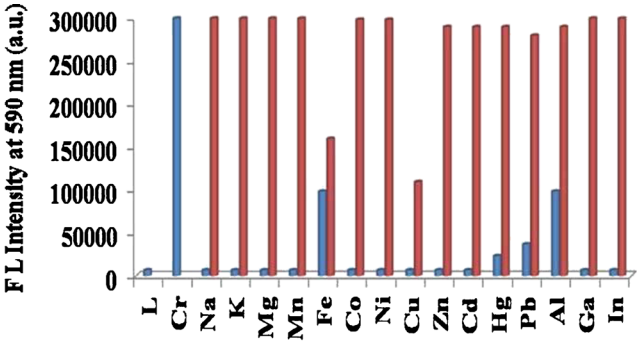


**Fig. 6** Metal ions selectivity of **RBNI** (10 μM) in 50 % (*v/v*) $H_2O/CH_3CN$ buffered by 10 mM HEPES pH 7.2 at 25 °C. *Blue bars*: fluorescence intensity of **RBNI** with the addition of the respective cations (100 μM). Maroon bars: fluorescence intensity of **RBNI** with the addition of the respective competing cations (100 μM) and $Cr^{3+}$ (100 μM). The fluorescence intensities were detected at 590 nm

obtained in case of chemosensor **RBNI**, as well as $Cr^{3+}$-bound form can be fitted to a triexponential functions and the relevant data were compiled in Table S1 (in Supplementary data). The minor and short-lived component was assigned to the decay time for the excited state related to the spirolactam moiety, while the long-lived major component was attributed to the xanthene form of the chemosensor **RBNI**. The relative increase in the percentage of the open-ring xanthene form upon addition of $Cr^{3+}$ confirms the interaction of $Cr^{3+}$ with the receptor.

The spirolactam ring of the rhodamine moiety in **RBNI** is susceptible to change in pH. Experimental results show that, for free **RBNI**, at acidic conditions (pH<5), an obvious off–on fluorescence appeared due to the formation of the open-ring state because of the strong protonation (Fig. 9). Therefore, we evaluated the fluorescence properties of **RBNI** in solutions with different pH values (2–14). It was found that the fluorescence intensity of the probe remains stable in the pH range 5–14. Upon the addition of $Cr^{3+}$ ions, there was an obvious fluorescence off–on change of **RBNI** under different pH values. Thus, the sensor **RBNI** has the maximal sensing response at physiological pH, indicating that the sensor **RBNI** is promising for biological applications.

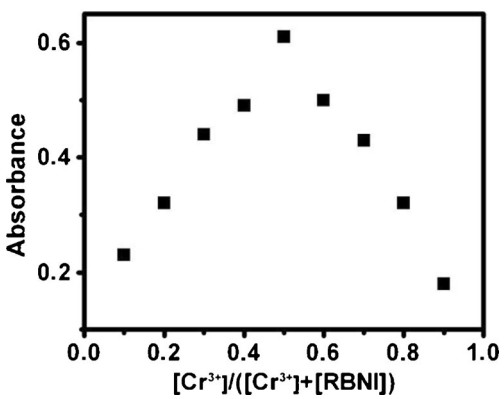


**Fig. 7** Job plot of **RBNI** and $Cr^{3+}$ ([**RBNI**] + [$Cr^{3+}$] = 45 μM) in 50 % (*v/v*) $H_2O/CH_3CN$ buffered by 10 mM HEPES at pH 7.2 at 25 °C

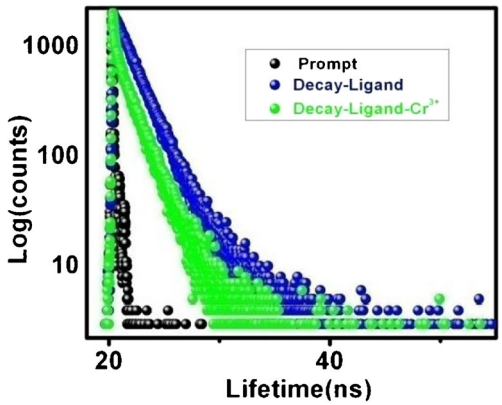


**Fig. 8** Time-resolved fluorescence decay of **RBNI** (*blue*), Prompt (*black*) and **RBNI**-$Cr^{3+}$ (*green*)

## $^1$H NMR Titration

For further insight into the binding event of **RBNI** with $Cr^{3+}$, we performed $^1$H NMR titration experiment by the addition of 1 equiv. of $Cr^{3+}$ to **RBNI** (Fig. 10). Upon addition of $Cr^{3+}$, the peak shape of **RBNI** broadened and almost all aromatic protons shifted downfield. This indicates that the opening of the spirolactum ring in **RBNI** was occurred in the presence of $Cr^{3+}$. Further, IR spectrum of chemosensor **RBNI** with $Cr^{3+}$ ion also confirms the proposed mechanism (Fig. S13, in Supplementary data). Upon addition of 1 equiv. of $Cr^{3+}$, the characteristic carbonyl amide stretching frequency shifts from 1701 $cm^{-1}$ in **RBNI** to 1587 $cm^{-1}$ in the complex, indicating coordination of carbonyl oxygen with $Cr^{3+}$ ion. These findings clearly support the ring-opening mechanism.

In order to examine the reliability of our sensing system, practical application was evaluated by determining the recoveries of spiked $Cr^{3+}$ in pond water and tap water samples, respectively. The samples collected were simply pretreated with filtration before further determination. No $Cr^{3+}$ was found in these water samples. Then $Cr^{3+}$ stock solution was separately spiked in these samples and **RBNI** probe was

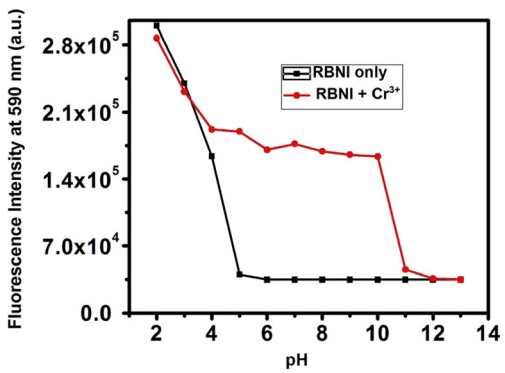


**Fig. 9** Variation of fluorescence intensity (590 nm) of free **RBNI** (10 μM) and in the presence of 100 μM $Cr^{3+}$ ion in 50 % (*v*/*v*) $H_2O$/$CH_3CN$ buffered by 10 mM HEPES at pH 7.2 at 25 °C, solution with different pH conditions

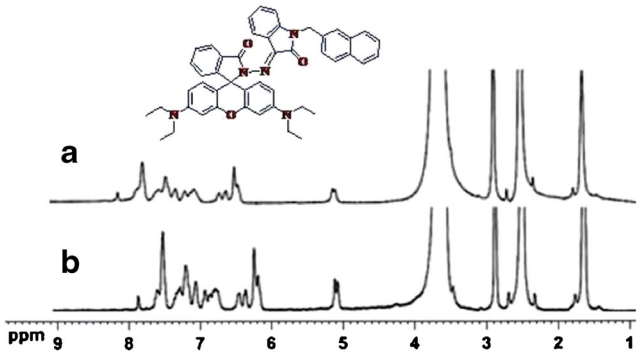


**Fig. 10** $^1$H NMR titration of **RBNI** and with $Cr^{3+}$ ion (DMSO-$d_6$, 300 MHz); **a RBNI** only **b RBNI** with 1 equiv. of $Cr^{3+}$

employed to detect its concentration. The results were summarized in Table S2 (Supplementary data), which showed satisfactory recovery values for all of the samples. Thus, the present probe seems useful for the determination of $Cr^{3+}$ in natural water samples.

## Conclusion

In summary, we have designed and synthesized a novel rhodamine-based chromo-/fluorogenic dual signalling probe for selective recognition of $Cr^{3+}$ in aqueous $CH_3CN$ media. It has been well characterized by various spectroscopic techniques. The colorimetric and fluorescent response to $Cr^{3+}$ can be conveniently detected even by the naked eye, which provides a facile method for visual detection of $Cr^{3+}$. Upon the addition of $Cr^{3+}$, the spirolactam ring of **RBNI** was opened and a 1:1 metal-ligand complex was formed. All biologically relevant metal ions and toxic heavy metals did not interfere with the $Cr^{3+}$ ion detection with this sensor. The excellent detection limit (2.4 μM) of **RBNI** chemosensor toward $Cr^{3+}$ ion can be used for the detection of trace quantities of $Cr^{3+}$ ion in biological and environmental sample. We believe that the sensor can be used for practical applications in chemical, environmental and biological systems.

**Acknowledgments** A.D. thanks to CSIR, New Delhi, India for financial support by awarding senior research fellowship (Sanc. No. 01(2401)/10/EMR-II, dated 05.01. 2011).

## References

1. Manez RM, Sancenon F (2003) Fluorogenic and chromogenic chemosensors and reagents for anions. Chem Rev 103:4419–4476
2. Czarnik AW (1994) Chemical communication in water using fluorescent chemosensors. Acc Chem Res 27:302–308
3. Kim JS, Quang DT (2007) Calixarene-derived fluorescent probes. Chem Rev 107:3780–3799

4. Sinkeldam RW, Greco NJ, Tor Y (2010) Fluorescent analogs of biomolecular building blocks: design, properties, and applications. Chem Rev 110:2579–2619
5. Czarnik AW (1992) Fluorescent chemosensors for ion and molecule recognition. Ed. American Chemical Society, Washington, DC
6. Numata M, Li C, Bae AH, Kaneko K, Sakurai K, Shinkai S (2005) β-1,3-Glucan polysaccharide can act as a one-dimensional host to create novel silica nanofiber structures. Chem Comm 4655–4657
7. Henry A (1968) The role of chromium in mammalian nutrition. J Nutr 21:230–244
8. Gómez V, Callao MP (2006) Chromium determination and speciation since 2000 trends. Anal Chem 25:1006–1015
9. Latva S, Jokiniemi J, Peraniemi S, Ahlgren M (2003) Separation of picogram quantities of Cr(III) and Cr(VI) species in aqueous solutions and determination by graphite furnace atomic absorption spectrometry. J Anal At Spectrom 18:84–86
10. Arakawa H, Ahmad R, Naoui M, TaJmir-Riahi HA (2000) A comparative study of calf thymus DNA binding to Cr(III) and Cr(VI) ions evidence for the guanine N-7-chromium-phosphate chelate formation. J Biol Chem 275:10150–10153
11. Li Z, Zhao W, Zhang Y, Zhang L, Yu M, Liu J, Zhang H (2011) An 'off-on' fluorescent chemosensor of selectivity to $Cr^{3+}$ and its application to MCF-7 cells. Tetrahedron 67:7096–7100
12. Vincent JB (2000) Quest for the molecular mechanism of chromium action and its relationship to diabetes. Nutr Rev 58:67–72
13. Bencheikh-Latmani R, Obraztsova A, Mackey MR, Ellisman MH, Tebo BM (2006) Toxicity of Cr(III) to *Shewanella* sp. strain MR-4 during Cr(VI) reduction. Environ Sci Technol 41:214–220
14. Mahmoud ME, Yakout AA, Ahmed SB, Osman MM (2008) Development of a method for chromium speciation by selective solid phase extraction and preconcentration on alumina-functionalized thiosemicarbazide. J Liq Chromatogr Relat Technol 31:2475–2492
15. (1989) National research council, recommended dietary allowance, Tenth Edition. National Academy Press, Washington, D. C.
16. Costa M, Klein CB (2006) Toxicity and carcinogenicity of chromium compounds in humans. CRC Crit Rev Toxicol 36:155–163
17. Dai R, Yu C, Liu J, Lan Y, Deng B (2010) Photo-oxidation of Cr(III)-citrate complexes forms harmful Cr(VI). Environ Sci Technol 44:6959–6964
18. O'Brien T, Mandel HG, Pritchard DE, Patierno SR (2002) Critical role of chromium (Cr)-DNA interactions in the formation of Cr-induced polymerase arresting lesions. Biochemistry 41:12529–12537
19. Arar EJ, Paff JO (1991) Determination of dissolved hexavalent chromium in industrial wastewater effluents by ion chromatography and post-column derivatization with diphenylcarbazide. J Chromatogr 546:335–340
20. Ososkov V, Kebbekus B, Chesbro D (1996) Field determination of Cr(VI) in water at low ppb level. Anal Lett 29:1829–1850
21. Varnes AW, Dodson RB, Wehry EL (1972) Interactions of transition-metal ions with photoexcited states of flavines. Fluorescence quenching studies. J Am Chem Soc 94:946–950
22. Zhou Y, Zhang J, Zhang L, Zhang Q, Ma T, Niu J (2013) A rhodamine-based fluorescent enhancement chemosensor for the detection of $Cr^{3+}$ in aqueous media. Dyes Pigments 97:148–154
23. Wan Y, Guo Q, Wang X, Xia A (2010) Photophysical properties of rhodamine isomers: a two-photon excited fluorescent sensor for trivalent chromium cation ($Cr^{3+}$). Anal Chim Acta 665:215–220
24. Huang K, Yang H, Zhou Z, Yu M, Li F, Gao X, Yi T, Huang C (2008) Multisignal chemosensor for $Cr^{3+}$ and its application in bioimaging. Org Lett 10:2557–2560
25. Zhou Z, Yu M, Yang H, Huang K, Li F, Yi T, Huang C (2008) FRET-based sensor for imaging chromium(III) in living cells. Chem Commun 3387–3389
26. Rurack K, Kollmannsberger M, Resch-Genger U, Daub J (2000) A Selective and sensitive fluoroionophore for HgII, AgI, and CuII with virtually decoupled fluorophore and receptor units. J Am Chem Soc 122:968–969
27. Resendiz MJE, Noveron JC, Disteldorf H, Fischer S, Stang PJ (2004) A self-assembled supramolecular optical sensor for Ni(II), Cd(II), and Cr(III). Org Lett 6:651–653
28. Zyryanov GV, Palacios MA, Anzenbacher P (2007) Rational design of a fluorescence-turn-on sensor array for phosphates in blood serum. Angew Chem Int Ed 46:7849
29. Zhang M, Yu M, Li F, Zhu M, Li M, Gao Y, Li L, Liu Z, Zhang J, Zhang D (2007) A highly selective fluorescence turn-on sensor for cysteine/homocysteine and its application in bioimaging. J Am Chem Soc 129:10322–10323
30. Kim H, Lee M, Kim H, Kim J, Yoon J (2008) A new trend in rhodamine-based chemosensors: application of spirolactam ring-opening to sensing ions. Chem Soc Rev 37:1465–1472
31. Liu H, Wan X, Liu T, Li Y, Yao Y (2014) Cascade sensitive and selective fluorescence OFF-ON-OFF sensor for $Cr^{3+}$ cation and $F^-$ anion. Sensors Actuators B 200:191–197
32. King CIM, Bergh JJ, Petzer JP (2011) Inhibition of monoamine oxidase by selected $C_5$- and $C_6$-substituted isatin analogues. Bioorg Med Chem 19:261–274
33. Jiang Y, Hansen TV (2011) isatin 1,2,3-triazoles as potent inhibitors against caspase-3. Bioorg Med Chem Lett 21:1626–1629
34. Burdette SC, Lippard SJ (2001) ICCC34—golden edition of coordination chemistry reviews. Coordination chemistry for the neurosciences. Coord Chem Rev 216:333–361
35. Prodi L (2005) Luminescent chemosensors: from molecules to nanoparticles. New J Chem 29:20–31
36. Dhara A, Jana A, Konar S, Ghatak SK, Ray S, Das K, Bandyopadhyay A, Guchhait N, Kar SK (2013) A novel rhodamine-based colorimetric chemodosimeter for the rapid detection of $Al^{3+}$ in aqueous methanol: fluorescent 'OFF–ON' mechanism. Tetrahedron Lett 54:3630–3634
37. Dhara A, Jana A, Guchhait N, Ghosh P, Kar SK (2014) Rhodamine-based molecular clips for highly selective recognition of $Al^{3+}$ ions: synthesis, crystal structure and spectroscopic properties. New J Chem 38:1627–1634
38. Dhara A, Jana A, Guchhait N, Kar SK (2014) Isatin appended rhodamine scaffold as an efficient chemical tool to detect selectively $Al^{3+}$. J Lumin 154:369–375
39. Anthoni U, Christophersen C, Nielsen P, Puschl A, Schaumburg K (1995) structure of red and orange fluorescein. Struct Chem 3:161–165
40. Xiang Y, Tong A, Jin P, Ju Y (2006) New fluorescent rhodamine hydrazone chemosensor for Cu(II) with high selectivity and sensitivity. Org Lett 8:2863–2866
41. Lakowicz JR (1999) Principles of fluorescence spectroscopy. Plenum, New York
42. Kubin RF, Fletcher AN (1952) Fluorescence quantum yields of some rhodamine dyes. J Lumin 27:455–462
43. Bhattacharya B, Nakka S, Guruprasad L, Samanta A (2009) Interaction of bovine serum albumin with dipolar molecules: fluorescence and molecular docking studies. J Phys Chem B 113:2143–2150
44. Teuchner K, Pfarrherr A, Stiel H, Freyera W, Leupold D (1993) Spectroscopic properties of potential sensitizers for new photodynamic therapy start mechanisms via two-step excited electronic states. Photochem Photobiol 57:465–471
45. Stiel H, Teuchner K, Paul A, Freyer W, Leupold DJ (1994) Two-photon excitation of alkyl-substituted magnesium phthalocyanine: radical formation via higher excited states. Photochem Photobiol A 80:289–298
46. Long GL, Winefordner JD (1983) Limit of detection a closer look at the IUPAC definition. Anal Chem 55:712A–724A
47. Kaur M, Kaur P, Dhuna V, Singh S, Singh K (2013) A ferrocene-pyrene based 'turn-on' chemodosimeter for $Cr^{3+}$ - application in bioimaging. Dalton Trans 43:5707–5712

48. Wu S, Zhang K, Wang Y, Mao D, Liu X, Yu J, Wang L (2014) A novel $Cr^{3+}$ turn-on probe based on naphthalimide and binol framework. Tetrahedron Lett 55:351–353
49. EPA US (1999) Integrated Risk Information System (IRIS) on chromium III. National Center for Environmental Assessment. Office of Research and Development, Washington
50. Vosburgh WC, Copper GR (1941) The identification of complex ions in solution by spectrophotometric measurements. J Am Chem Soc 63:437–442
51. Benesi HA, Hildebrand JH (1949) A spectrophotometric investigation of the interaction of iodine with aromatic hydrocarbons. J Am Chem Soc 71:2703–2707